International Journal of Remote Sensing
Vol. 31, No. 13, 10 July 2010, 3535–3543

Taylor & Francis
Taylor & Francis Group

Co-seismic ionospheric and deformation signals on the 2008 magnitude 8.0 Wenchuan Earthquake from GPS observations

SHUANGGEN JIN*†‡§, W. ZHU† and E. AFRAIMOVICH¶
†Shanghai Astronomical Observatory, Chinese Academy of Sciences, Shanghai 200030, China
‡Korea Astronomy and Space Science Institute, Daejeon 305-348, South Korea
§Center for Space Research, University of Texas at Austin, TX 78759, USA
¶Institute of Solar-Terrestrial Physics, SB RAS, Irkutsk 664033, Russia

The 8.0 magnitude Wenchuan Earthquake occurred at the Longmenshan Fault along the eastern boundary between the Tibetan Plateau and the western Sichuan Basin in southwestern China on 12 May 2008, killing tens of thousands of people in several cities along the western Sichuan Basin. In this paper, co-seismic ionospheric and deformation signals from the mainshock of this event are extracted from national global positioning system (GPS) network observations, which provide unique insights into this event. The co-seismic deformation moves towards the earthquake epicentre, and the largest magnitude reaches 2.3 m in Beichuan. The total moment of the co-seismic rupture is 2.4×10^{21} nm, equivalent to a magnitude of 8.1 and nearly identical to the seismological estimate. Furthermore, co-seismic ionospheric disturbances indicate a shock-acoustic wave propagation at a mean velocity of about 600 m s^{-1} towards the rupture direction.

1. Introduction

The 12 May 2008 earthquake with a magnitude of 8.0 occurred at 06:28 UT in Wenchuan County (31.0° N, 103.4° E), 80 km west/northwest of the provincial capital city of Chengdu, killing ten of thousands of people in several cities along the western Sichuan Basin in China (figure 1). The extent of the Wenchuan Earthquake and after shock-affected areas lay north-east, along the Longmenshan Fault. The Longmenshan Fault is a thrust fault with a strike fault plane approximately north-east, running along the eastern boundary between the Tibetan Plateau and the western Sichuan Basin in southwestern China (Jia *et al.* 2006). The motion of the Longmenshan Fault causes the uplift of the Longmen Mountain relative to the lowlands of the Sichuan Basin to the east. In the past, the Longmenshan Fault had a mostly right-lateral strike-slip and a smaller amount of thrust motion (Densmore *et al.* 2007). Furthermore, the Longmenshan Fault has a late-Cenozoic deformation in the Guanxian-Jiangyou, Yingxiu-Beichuan fracture and Wenchuan-Mao County fracture as well as their related folds, which was possibly a result of the Longmenshan thrust pushing southeastwards combined with clockwise shears. However, the geological structures along the Longmenshan suggest a total displacement by tens of kilometres since the Late Cenozoic and its long-term slip rate is slower than 1 mm per year (Ly *et al.* 2006, Densmore *et al.* 2007). Furthermore, present-day global positioning system (GPS)

*Corresponding author. Email: sgjin@csr.utexas.edu; shuanggen.jin@gmail.com

International Journal of Remote Sensing
ISSN 0143-1161 print/ISSN 1366-5901 online © 2010 Taylor & Francis
http://www.tandf.co.uk/journals
DOI: 10.1080/01431161003727739

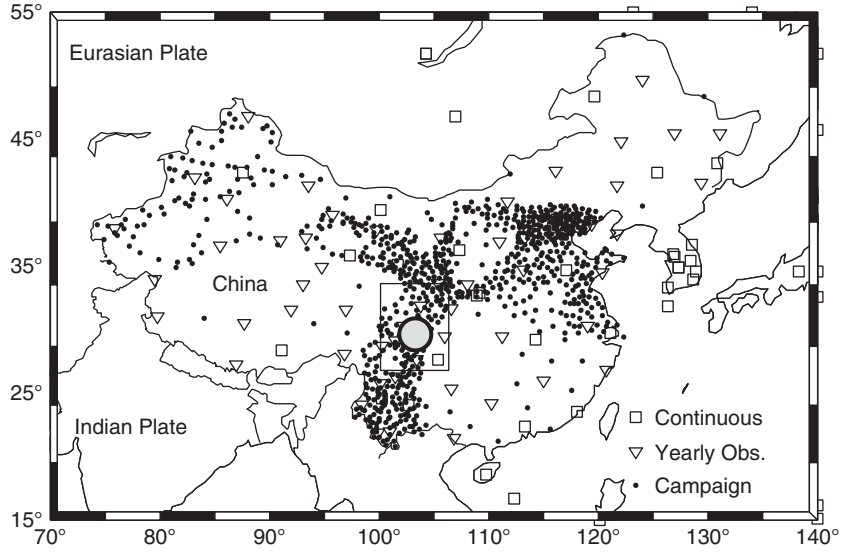

Figure 1. Map of eastern Asia, global positioning system (GPS) observation network and the epicentre of the 12 May 2008 Wenchuan Earthquake mainshock of magnitude 8.0. Squares are the continuous GPS observing sites, triangles are the yearly observing GPS sites and dots are the campaign GPS sites. The large solid circle is the epicentre of this event mainshock.

observations confirm the current structural deformation of the Longmenshan characterized by thrust and right-handed shears with a low deformation rate of a few millimetres per year (Meade 2007, Royden *et al.* 2008), but the processes of driving deformation are still very much in debate (Burchfiel *et al.* 1995, Chen *et al.* 2000, Densmore *et al.* 2007, Sol *et al.* 2007, Royden *et al.* 2008). Therefore, the violent earthquake of magnitude 8.0 that occurred at the Longmenshan Fault Zone was not expected, resulting in one of the largest death tolls during the last century as well as geological damage.

This event ruptured about 300 km of the Longmenshan Fault Zone and lasted for 110–120 s (Burchfiel *et al.* 2008, Parsons *et al.* 2008, Toda *et al.* 2008). The rupture started from Wenchuan and propagated at an average speed of 3.1 km s^{-1}, 49° towards the northeast with a total of about 300 km (http://www.csi.ac.cn). The estimates of the size of the earthquake from seismic data are highly sensitive to the method and frequency band used in the analysis. For example, the magnitude scale of this mainshock was 7.9 ($M_0 = 9.43 \times 10^{20}$Nm) from the Harvard CMT estimate (http://www.globalcmt.org/), and 8.0 from the China Earthquake Administration (http://www.csi.ac.cn). Although robust seismic signals around the globe could estimate the gross nature of this event, the details of rupture are usually obscure due to the lack of near-field observations. Geodetic measurements can be used to calculate the kinematic rupture and the size of the earthquake as well as ionospheric disturbances, which provide unique insights into the details of continental events. In this paper, dense GPS network observation data are collected from China national continuous and campaign GPS networks, and the co-seismic deformation and ionospheric disturbances are investigated for this event.

2. GPS observation data

In August 1998, the national project Crustal Movement Observation Network of China (CMONC) was initiated (Jin *et al.* 2007). The network provides data from a nationwide fiducial network of 25 continuous GPS sites observed from August 1998 to present, and data from 56 survey mode sites with yearly occupations for the period 1998–2008. They also include ~1000 regional campaign GPS stations operated by the State Bureau of Surveying and Mapping (SBSM) and China Earthquake Administration (CEA) in 1999, 2001, 2004, 2007 and 2008. These campaign GPS sites were observed continuously for at least 4 days during each session. All the sites are shown in figure 1. Squares show the continuous GPS observing sites, triangles are the yearly observing GPS sites and dots show the campaign GPS sites. The large solid circle is the epicentre of this mainshock.

3. GPS data processing and results

The GPS consists of a constellation of 24 operating satellites in six circular orbits 20 200 km above the Earth, at an inclination angle of 55° with a 12-h period. The satellite transmits two frequencies of signals ($f_1 = 1575.42$ MHz and $f_2 = 1227.60$ MHz). The equations of carrier phase (L) and code observations (pseudorange P) of double frequency GPS can be expressed as follows:

$$L^i_{k,j} = \lambda_k \phi^i_{k,j} = \left|\vec{r}^{\,i} - \bar{r}_j\right| - d^i_{ion,k,j} + d^i_{trop,j} + c(\tau^i - \tau_j) - \lambda_k(b^i_{k,j} + N^i_{k,j}) \tag{1}$$

$$P^i_{k,j} = \left|\vec{r}^{\,i} - \bar{r}_j\right| + d^i_{ion,k,j} + d^i_{trop,j} + c(\tau^i - \tau_j) + d^i_{q,k} + d_{q,k,j} + \varepsilon^i_j \tag{2}$$

where k is the frequency ($k = 1, 2$), superscript i and subscript j represent the satellite and ground-based GPS receiver, respectively, $\vec{r}^{\,i}$ is the position of satellite i; $\vec{r}_j$is the coordinate of GPS receiver j; d_{ion} and d_{trop} are the ionospheric and tropospheric delays, respectively; c is the speed of light in vacuum space; τ is the satellite or receiver clock offset; b is the phase delay of the satellite and receiver instrument bias; d_q is the code delay of the satellite and receiver instrumental bias; λ is the carrier wavelength; ϕ is the total carrier phase between the satellite and the receiver; N is the ambiguity of the carrier phase; and ε is the other residuals. With more than four satellite observations, the unknown parameters (e.g. GPS receiver coordinate and tropospheric delays) and their uncertainties can be obtained using the least square (LS) method with some algorithms. These parameters may provide some insights into geological and atmospheric events, such as earthquakes, volcanoes, subsidence, meteorology and space weather.

3.1 *Co-seismic ionospheric disturbance*

Since the ionosphere is a dispersive medium, dual frequency GPS receivers are able to estimate the total ionospheric delay or eliminate the ionospheric delay effect with measurement of the modulations on the pseudoranges and the carrier phases. After combining the dual frequency pseudorange and carrier phase observations, the slant total electron content (TEC) can be obtained and then transferred into the vertical TEC (Jin *et al.* 2008). At time t, each ith element of the vertical TEC is denoted by the measured TEC value $I_i(t)$. The duration of the TEC time series depends on the time span when the GPS-satellite is in the zone of a corresponding receiver's radio visibility. TEC time series reflect regular changes of the ionosphere and abnormal variations caused by irregularities of electron concentration of various scales, such as

geological events due to the coupling of the solid-Earth and the ionosphere. We here filtered the TEC series $dI(t)$ by removing the trend with a time window of 5–20 min in order to show characteristic ionospheric disturbances. Significant ionospheric disturbances are found at continuous GPS sites within 500 km from the epicentre. We checked the solar activity indices (e.g. Auroral Electrojet (AE) and $F_{10.7}$ cm solar radio flux) and geomagnetic indices (e.g. Kp and Dst) and found that the day of 12 May 2008 was a geomagnetically quiet day. Therefore, these co-seismic ionospheric characteristics mainly reflect the coupling of the ionosphere and Wenchuan Earthquake. For example, figure 2 shows the significant TEC variations at KUNM station during the mainshock, indicating a significant co-seismic ionospheric disturbance. Here the ionospheric pierced points used are from satellites PRN14, PRN22, PRN05 and PRN18 at time t_{max} of maximum TEC response on main earthquake shock for line-of-site KUNM (figure 3).

In order to determine propagation dynamics of the ionospheric disturbance, a simple interferometric method D1 (Afraimovich *et al.* 2001) and the quasi-optimum algorithm (QOA) method (Kiryushkin and Afraimovich 2007) are used to determine the angular characteristics of the wave vector and phase velocity of ionospheric disturbances due to the Wenchuan Earthquake. We found that intensive N-shaped shock-acoustic waves with a plane waveform and with a half-period of about 200 s propagated towards the northeast with a mean velocity of 600 m s^{-1} for a distance of about 1000 km from the epicentre, in parallel with the rupture direction. For a more

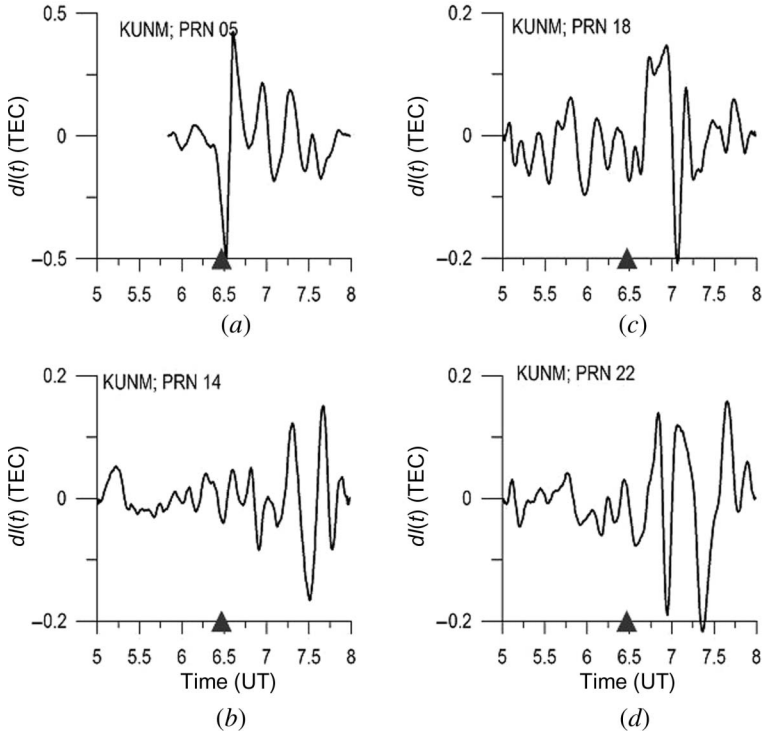

Figure 2. Filtered total electron content (TEC) series $dI(t)$ for KUNM-PRN05 (*a*), PRN14 (*b*), PRN18 (*c*) and PRN22 (*d*). The time of the Wenchuan Earthquake mainshock is marked by a triangle.

detailed description of methods and results, see Afraimovich *et al.* (2010). In the future, we will further investigate the coupling processes and mechanism of the seismo-ionospheric TEC variations.

3.2 *Co-seismic deformations*

All available GPS data were processed in 24-h segments (0–24 GMT) with the GAMIT/GLOBK software package (Herring 2002, King and Bock 2002). At the first step, we applied loose *a priori* constraints to all parameters and used double-difference GPS observations with the ionosphere-free combination algorithm from each day to estimate station coordinates, the zenith tropospheric delay (ZTD) at each station every 2 hours, and the orbital and Earth rotation parameter (ERP). We use International GNSS Service (IGS) final orbits, International Earth Rotation and Reference Systems Service (IERS) Earth orientation parameters, and apply azimuth- and elevation-dependent antenna phase centre models, following the tables recommended by the IGS. Secondly, regional daily solutions were combined with global IGS network solutions produced routinely by the Scripps Orbital and Position Analysis Center (SOPAC, http://sopac.ucsd.edu/) using the GLOBK software, and the reference frame is applied to the solution by performing a seven-parameter transformation to align it to ITRF2005 with 57 global core stations (Altamimi *et al.* 2007). For example, figure 4 is the coordinate time series residual at H035 site, showing a co-seismic deformation of about 2 m in the horizontal and 1 m in the vertical. To estimate co-seismic displacements at all continuous and campaign GPS sites, we used a simple, linear-in-time model for elastic strain accumulation to extrapolate the station position measured before the earthquake to the time immediately preceding the shock. Stations more than 350 km from the epicentre were displaced by

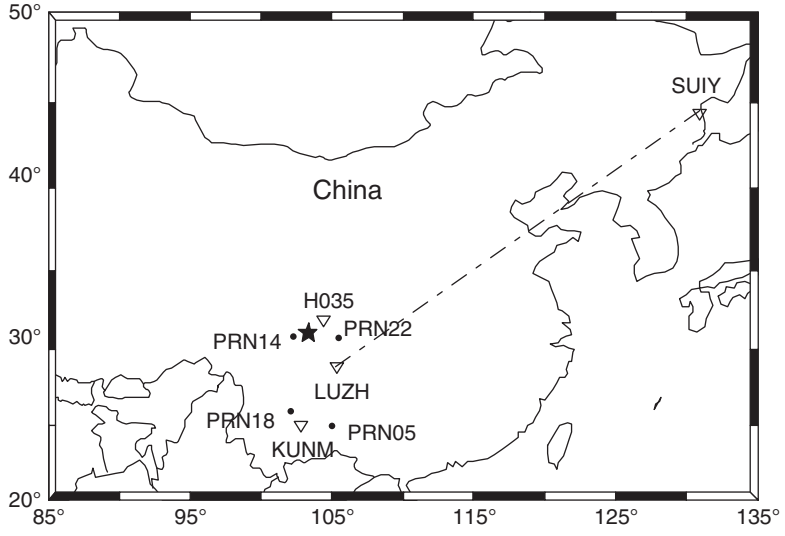

Figure 3. Locations of selected experimental global positioning system (GPS) sites and satellite pierced points during the Wenchuan Earthquake. The star shows the location of the epicentre mainshock, triangles denote the GPS sites, and dots represent the ionospheric pierced points of satellites PRN14, PRN22, PRN05 and PRN18 at time t_{max} of maximum total electron content response on earthquake mainshock for used line-of-site KUNM.

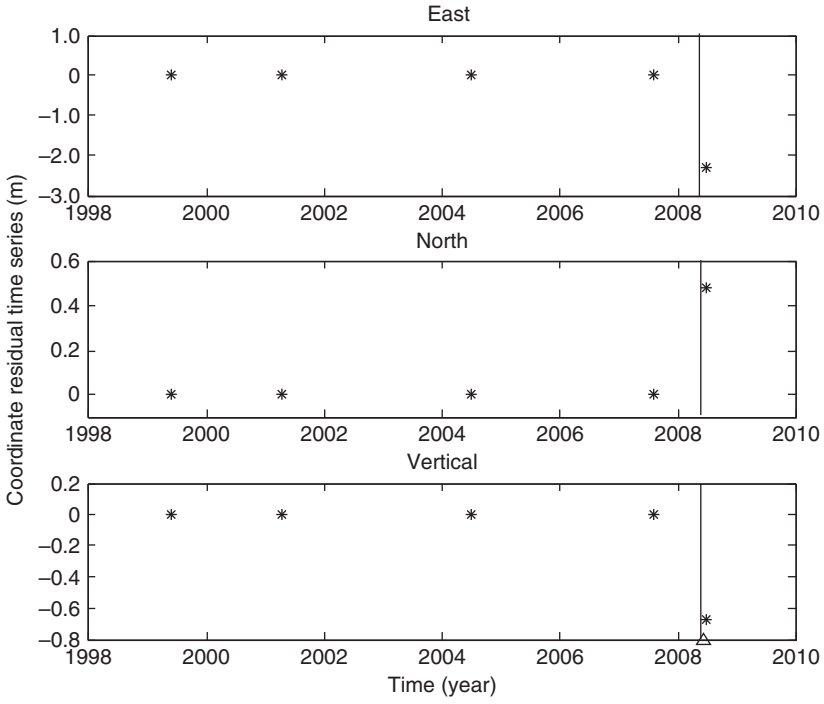

Figure 4. Global positioning system (GPS) coordinate residual time series at site H035. The vertical line shows the mainshock time of the Wenchuan Earthquake.

less than 10 mm. However, far-field GPS baseline solutions show clear shocks with amplitudes of about 2 cm from this event. For example, figure 5 shows the long baseline length time series of LUZH-SUIY (see figure 3) at 30 s intervals from 06:00 UT to 07:00 UT, indicating a co-seismic displacement disturbance of about 1–3 cm. Significant co-seismic displacements of GPS sites near the epicentre are shown in figure 6. It can be seen that the coherent surface motion roughly directed towards the earthquake ruptures at distances up to 350 km from the epicentre. Overall, the co-seismic deformations move towards the earthquake epicentre. North–south trending displacements in Wenchuan (between 31.0° and 31.5°) and east–west trending

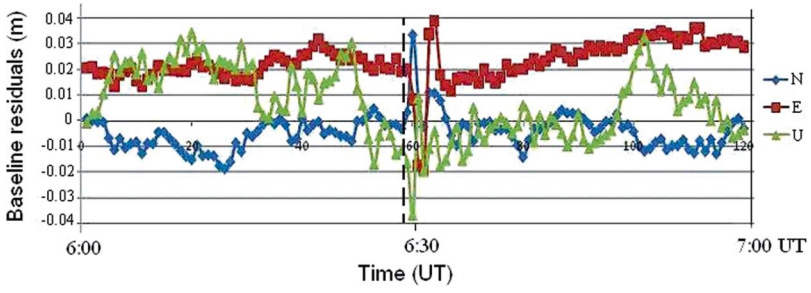

Figure 5. Long baseline length residual time series (m) of LUZH-SUIY at 30 s intervals from 06:00 UT to 07:00 UT. The mainshock of the Wenchuan Earthquake is at 06:28 UT, marked by a dashed line.

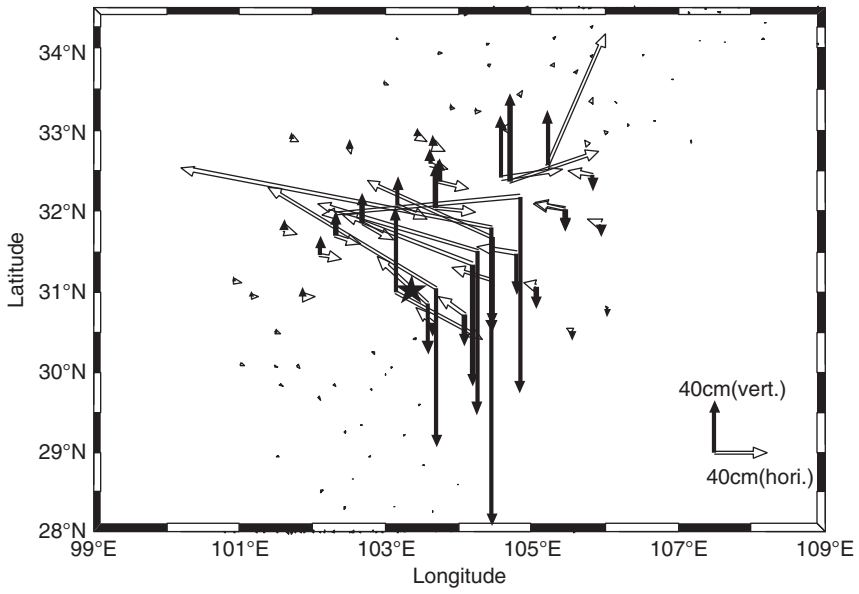

Figure 6. Map view of co-seismic displacements for the 12 May 2008 Wenchuan Earthquake. Horizontal displacements from global positioning system (GPS) data are the blank arrows and vertical displacements are shown as solid black arrows. The epicentre of the May 2008 main-shock is shown as a black star.

displacements in Qingchuan (between 31.5° and 32.0°) are mainly due to a thrust focal mechanism, aligned with the Longmenshan Fault zone. The larger co-seismic displacements are in Dujiangyan-Wenchuan, Qingchuan and Beichuan Counties, while the largest magnitude is up to 2.3 m in the horizontal and 0.7 m in the vertical in Beichuan rather than in the epicentre.

The co-seismic ruptures are further inverted using the elastic half-space homogeneous model with a homogeneous layered fault model (Okada 1985). The inversion results show that the non-constrained fault slip is most in accordance with the GPS observed co-seismic deformation and the seismic fault is not only right-lateral and thrust slip, but also with a little left-lateral slip and normal slip slide. The moment tensor is about 2.4×10^{21} nm, equivalent to a magnitude of 8.1 and nearly identical to the seismological estimate (http://earthquake.usgs.gov/eqcenter). The main forwardly-inverted co-seismic deformations are in Dujianyan-Wenchuan County and also in Beichuan, Qingchuan areas at the greatest deformation of about 4.5 m in the east direction and 0.8 m in the north direction with a strongly right-lateral characteristic, which is almost consistent with the wide geological surveying results.

Due to the extrusion of the Indian Plate to the Eurasian Plate and the Longmenshan's southeast push with the Sichuan Basin, the inter-plate relative motion might result in a thinning of the Qinghai-Tibet Plateau crust, the uplift of its landscape and an eastward extrusion. While near the Sichuan Basin, the east-northward motion of the Qinghai-Tibet Plateau meets with a strong resistance from the Yangtze Block, resulting in a strong strain accumulation in the Longmenshan Fault (Burchfiel *et al.* 1995, Densmore *et al.* 2007). This accumulated energy finally released and caused a sudden dislocation in the Yingxiu-Beichuan fracture, leading to

the violent earthquake of magnitude 8.0. Based on the largest co-seismic rupture of 2.3 m for this event and GPS measurements of the slip rate across the entire Longmenshan Fault Zone at less than 2 mm per year, the recurrence intervals of such great earthquakes can be deduced as about 1100 years. Therefore, this great Wenchuan Earthquake was characterized by a slow strain accumulation and long recurrence interval as well as huge devastating damage. Further studies should be dedicated to this new type of earthquake in the intra-plate in the future.

4. Conclusion

The 2008 Wenchuan Earthquake (magnitude 8.0) that occurred at the Longmenshan Fault Zone was very devastating, resulting in one of the largest death tolls in the last century as well as geological damage. The dense GPS network observation data collected from China national continuous and campaign GPS networks are used to investigate co-seismic ionospheric disturbances, co-seismic deformations, the size of the earthquake and surface wave propagations. The co-seismic deformations move towards the earthquake epicentre; the larger co-seismic deformations are in Wenchuan, Qingchuan and Beichuan Counties rather in the epicentre, while the largest magnitude is up to 2.3 m in Beichuan. The rupture model from co-seismic GPS displacements shows a total moment of 2.4×10^{21} nm, equivalent to a magnitude of 8.1 and nearly equivalent to the seismological estimate. Furthermore, GPS co-seismic TEC disturbances indicate a shock-acoustic wave propagation at a mean velocity of about 600 m s^{-1} in parallel with the rupture direction.

Acknowledgments

We are grateful to those who created the Crustal Motion Observation Network of China and made the observation data available and Dr Z. Li who provided some early GPS results. This work was supported by a grant from the Key Project of the Chinese Academy of Sciences, the Korea Research Council of Fundamental Science & Technology funded by the Ministry of Education, Science and Technology in 2009, the SB RAS and FEB RAS collaboration project N 3.24, the Interdisciplinary integral project of SB RAS N 56 'Seismoionospheric and Seismoelectromagnetic Processes in Baikal Rift Zone', the RFBR-GFEN grant no. 06-05-39026 and RFBR grant no. 07-05-00127.

References

Afraimovich, E.L., Perevalova, N.P., Plotnikov, A.V. and Uralov, A.M., 2001, The shock-acoustic waves generated by the earthquakes. *Annales Geophysicae*, **19**, pp. 395–409.

Afraimovich, E.L., Feng, D., Kirushkin, V., Astafyeva, E. and Jin, S.G., 2010, TEC response to the 2008 Wenchuan earthquake in comparison with other strong earthquakes. *International Journal of Remote Sensing*, **31**, pp. 3601–3613.

Altamimi, Z., Collilieux, X., Legrand, J., Garayt, B. and Boucher, C., 2007, ITRF2005: a new release of the International Terrestrial Reference Frame based on time series of station positions and Earth orientation parameters. *Journal of Geophysical Research*, **112**, B09401.

Burchfiel, B.C., Chen, Z., Liu, Y. and Royden, L.R., 1995, Tectonics of the Longmen Shan and adjacent regions, central China. *International Geological Review*, **37**, pp. 661–735.

Burchfiel, B.C., Royden, L.H., Van Der Hilst, R.D., Hager, B.H., Chen, Z., King, R.W., Li, C., Lü, J., Yao, H. and Kirby, E., 2008, A geological and geophysical context for the Wenchuan earthquake of 12 May 2008, Sichuan, People's Republic of China. *Geological Society of America Today*, **18**, pp. 4–11.

CHEN, Z., BURCHFIEL, B.C., LIU, Y., KING, R.W., ROYDEN, L.H., TANG, W., WANG, E., ZHAO, J. and ZHANG, X., 2000, Global Positioning System measurements from eastern Tibet and their implications for India/Eurasia intercontinental deformation. *Journal of Geophysical Research*, **105**, pp. 16215–16228.

DENSMORE, A.L., ELLIS, M.A., LI, Y., ZHOU, R., HANCOCK, G.S. and RICHARDSON, N., 2007, Active tectonics of the Beichuan and Pengguan faults at the eastern margin of the Tibetan Plateau. *Tectonics*, **26**, pp. TC4005.

HERRING, A., 2002, *GLOBK Global Kalman Filter VLBI and GPS Analysis Program, Version 10.0.* (Cambridge, MA: Massachusetts Institute of Technology Press).

JIA, D., WEI, G., CHEN, Z., LI, B., ZENG, Q. and YANG, G., 2006, Longmen Shan fold-thrust belt and its relation to the western Sichuan Basin in central China: new insights from hydrocarbon exploration. *AAPG Bulletin*, **90**, pp. 1425–1447, doi: 10.1306/03230605076.

JIN, S.G., ZHU, W. and PARK, P., 2007, Micro-plate tectonics and kinematics in Northeast Asia inferred from a dense set of GPS observations. *Earth and Planetary Science Letters*, **257**, pp. 486–496.

JIN, S.G., LUO, O.F. and PARK, P., 2008, GPS observations of the ionospheric F2-layer behavior during the 20th November 2003 geomagnetic storm over South Korea. *Journal of Geodesy*, **82**, pp. 883–892.

KING, R.W. and BOCK, Y., 2002, *Documentation for the GAMIT GPS Analysis Software* (Cambridge, MA: Massachusetts Institute of Technology Press).

KIRYUSHKIN, V.V. and AFRAIMOVICH, E.L., 2007, Determining the parameters of ionospheric perturbation caused by earthquakes with using the quasi-optimum algorithm of spatiotemporal processing of TEC measurements. *Earth, Planets and Space*, **59**, pp. 267–278.

LY, Y., ZHOU, R. and DENSEMORE, A., 2006, *Geodynamic Processes of the Eastern Margin of the Tibetan Plateau and its Geological Responses* (Beijing: Geological Publishing House).

MEADE, B.J., 2007, Present-day kinematics at the India-Asia collision zone. *Geology*, **35**, pp. 81–84.

OKADA, Y., 1985, Surface deformation due to shear and tensile faults in a half-space. *Bulletin of the Seismological Society of America*, **75**, pp. 1135–1154.

PARSONS, T., JI, C. and KIRBY, E., 2008, Stress changes from the 2008 Wenchuan earthquake and increased hazard in the Sichuan basin. *Nature*, **454**, pp. 509–510.

ROYDEN, L.H., BURCHFIEL, B.C. and VAN DER HILST, R.D., 2008, The geological evolution of the Tibetan Plateau. *Science*, **321**, pp. 1054–1058.

SOL, S., MELTZER, A., BURGMANN, R., VAN DER HILST, R.D., KING, R., CHEN, Z., KOONS, P., LEV, E., LIU, Y., ZEITLER, P.K., ZHANG, X., ZHANG, J. and ZUREK, B., 2007, Geodynamics of southeastern Tibet from seismic anisotropy and geodesy. *Geology*, **35**, pp. 563–566.

TODA, S., LIN, J., MEGHRAOUI, M. and STEIN, R.S., 2008, 12 May 2008 M = 7.9 Wenchuan, China, earthquake calculated to increase failure stress and seismicity rate on three major fault systems. *Geophysical Research Letters*, **35**, L17305.